

Dielectric, ferroelectric and field-induced strain behavior of $\text{K}_{0.5}\text{Na}_{0.5}\text{NbO}_3$ -modified $\text{Bi}_{0.5}(\text{Na}_{0.78}\text{K}_{0.22})_{0.5}\text{TiO}_3$ lead-free ceramics

Ali Hussain^{a,b,c}, Chang Won Ahn^b, Aman Ullah^b, Jae Shin Lee^d, Ill Won Kim^{b,*}

^a School of Nano and Advanced Materials Engineering, Changwon National University, Gyeongnam 641-773, Republic of Korea

^b Department of Physics and Energy Harvest-Storage Research Center, University of Ulsan, Ulsan 680-749, Republic of Korea

^c Faculty of Materials Science and Engineering, GIK Institute of Engineering Sciences and Technology, Topi 23640, KP, Pakistan

^d School of Materials Science and Engineering, University of Ulsan, Ulsan 680-749, Republic of Korea

Received 10 December 2011; received in revised form 26 January 2012; accepted 26 January 2012

Available online 4 February 2012

Abstract

Lead-free piezoelectric $(1-x)\text{Bi}_{0.5}(\text{Na}_{0.78}\text{K}_{0.22})_{0.5}\text{TiO}_3-x\text{K}_{0.5}\text{Na}_{0.5}\text{NbO}_3$ (BNKT– x KNN, $x=0$ –0.10) ceramics were synthesized using a conventional, solid-state reaction method. The effect of KNN addition on BNKT ceramics was investigated through X-ray diffraction (XRD), dielectric, ferroelectric and electric field-induced strain characterizations. XRD revealed a pure perovskite phase with tetragonal symmetry in the studied composition range. As the KNN content increased, the depolarization temperature (T_d) as well as maximum dielectric constant (ϵ_m) decreased. The addition of KNN destabilized the ferroelectric order of BNKT ceramics exhibiting a pinched-type hysteresis loop with low remnant polarization ($11 \mu\text{C}/\text{cm}^2$) and small piezoelectric constant ($27 \text{ pC}/\text{N}$) at 3 mol% KNN. As a result, at $x=0.03$ a significant enhancement of 0.22% was observed in the electric field-induced strain, which corresponds to a normalized strain ($S_{\text{max}}/E_{\text{max}}$) of $\sim 434 \text{ pm}/\text{V}$. This enhancement is attributed to the coexistence of ferroelectric and non-polar phases at room temperature.

© 2012 Elsevier Ltd and Techna Group S.r.l. All rights reserved.

Keywords: C. Dielectric response; Ferroelectrics; Piezoelectricity; Electrostriction; Order–disorder effects

1. Introduction

The development of lead-free piezoelectric ceramics have drawn considerable attention as a technological issue and environmental concern because of restrictions on the use of hazardous lead-based materials in electronic devices [1,2]. Much attention has been paid to bismuth sodium titanate $\text{Bi}_{0.5}\text{Na}_{0.5}\text{TiO}_3$ (BNT) and BNT-based solid solutions [3–10] because of their outstanding dielectric, ferroelectric and piezoelectric properties at compositions near the morphotropic phase boundary (MPB).

BNT has a perovskite-type structure with rhombohedral symmetry (R3C) at room temperature and a high Curie temperature (T_c) of approximately 320°C . However, these ceramics undergo another phase transition below T_c that is known as the depolarization temperature (T_d), which often

occurs below 200°C . In practice, T_d is a more important parameter than T_c because it is the operational limit of a BNT-based device. Additionally, BNT shows strong ferroelectricity ($P_r = 38 \mu\text{C}/\text{cm}^2$), but also has drawbacks such as a large coercive field of approximately $7.3 \text{ kV}/\text{mm}$ and a high conductivity, which leads to problems in the poling process [6,7]. To overcome these problems and optimize the properties of $\text{Bi}_{0.5}\text{Na}_{0.5}\text{TiO}_3$ solid solutions, investigations have concentrated on the search for a new MPB in BNT-based binary and ternary systems [6–10]. Among BNT-based solid solutions, the $\text{Bi}_{0.5}\text{Na}_{0.5}\text{TiO}_3$ – $\text{Bi}_{0.5}\text{K}_{0.5}\text{TiO}_3$ (BNT–BKT) system reported by Sasaki et al. [7] has a rhombohedral (F_R)–tetragonal (F_T) MPB at 16–20 mol% BKT and relatively high piezoelectric and ferroelectric properties at compositions near the MPB.

The alkaline niobate-based perovskite compound, $\text{K}_{0.5}\text{Na}_{0.5}\text{NbO}_3$ (KNN), is a well-known, lead-free piezoelectric ceramic with a high Curie temperature ($T_c = 420^\circ\text{C}$) and high electromechanical properties that has been studied as a possible substitute for lead-based piezoelectric ceramics [11–14]. Recently, Yao et al. [14] studied a BNT–BKT solid solution

* Corresponding author.

E-mail address: kimiw@mail.ulsan.ac.kr (I.W. Kim).

with the addition of a small amount (3 mol%) of KNN and observed a rhombohedral–tetragonal MPB with enhanced electromechanical properties. Seifert et al. [15] modified a MPB composition of 0.80BNT–0.20BKT with 0.97KNN–0.03BKT and reported a large strain at 1 mol% 0.97KNN–0.03BKT. However, detailed studies on the addition of KNN to BNT–BKT ceramics are limited and little is known about their dielectric properties, ferroelectric properties and temperature characteristics.

In this work, $(1-x)\text{Bi}_{0.5}(\text{Na}_{0.78}\text{K}_{0.22})_{0.5}\text{TiO}_3-x\text{K}_{0.5}\text{Na}_{0.5}\text{NbO}_3$ (BNKT– x KNN, $x=0$ –0.10) ceramics were synthesized by a conventional, solid-state reaction method and their crystal structure, microstructure, electrical properties (dielectric, ferroelectric and piezoelectric) and field-induced strain behavior were studied systematically.

2. Experimental

BNKT–KNN piezoelectric ceramics were fabricated by a conventional, solid-state reaction method using Bi_2O_3 , TiO_2 (99.9%, High Purity Chemical, Japan), Nb_2O_5 (99.5%, Cerac Specialty Inorganics, USA), Na_2CO_3 (99.9%, Cerac Specialty Inorganics, USA), and K_2CO_3 ($\geq 99\%$, Sigma–Aldrich, USA) as the starting raw materials. Prior to measuring the weight, the powders were dried in an oven at 100°C for 24 h. The dried powders were weighed according to the stoichiometric formula and ball-milled for 24 h in ethanol. The dried slurries were calcined at 800°C for 2 h, and then ball-milled again for 24 h. The powders were pulverized, passed through a sieve of $125\ \mu\text{m}$ mesh, mixed with an aqueous polyvinyl alcohol (PVA) solution as a binder for granulation, and then pressed into 13 mm-diameter pellets under 100 MPa of pressure. To prevent the loss of volatile Bi, Na, and K, the green pellets were embedded in the corresponding powders and sintered at 1150°C for 2 h in a covered alumina crucible.

The crystal structure of the sintered pallets was characterized with an X-ray diffractometer (XRD, X'pert PRO MRD, Philips) using $\text{Cu K}\alpha 1$ radiation. The surface morphology was observed with a field emission electron microscope (FE-SEM, JEOL, JSM-650FF, Japan). To measure the electrical properties, silver–palladium paste was electroded on both surfaces of the samples and fired at 700°C for 30 min. The dielectric constant and tangent loss of the poled specimens were measured using an impedance analyzer (HP4192A) attached to a programmable furnace at frequencies from 1 to 100 kHz over a temperature range of 30 – 500°C . The piezoelectric properties were measured using a Berlincourt meter after poling the samples with an electric field of $3\ \text{kV/mm}$ for 10 min at 80°C . The dependence of the electric polarization (P) and mechanical strain (S) under an external electric field (E) were measured in a silicon oil bath using a modified Sawyer–Tower circuit and a linear variable differential transducer (LVDT), respectively.

3. Results and discussion

Fig. 1 shows the XRD patterns of all sintered BNKT– x KNN ceramics in the 2θ range of 20 – 80° . The XRD patterns revealed

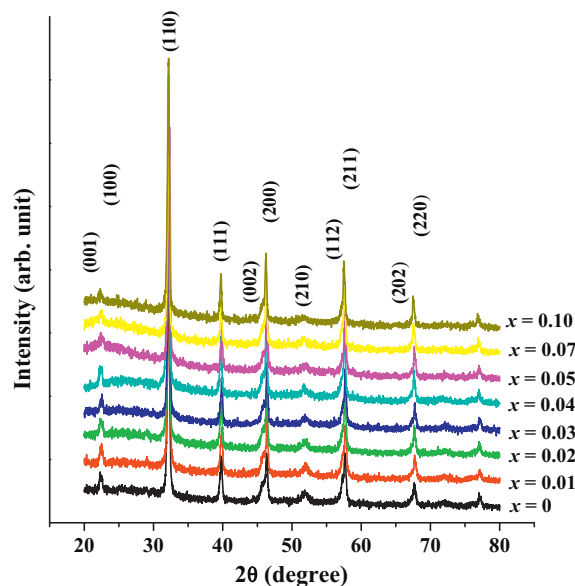


Fig. 1. X-ray diffraction patterns of BNKT– x KNN ceramics in the 2θ range of 20 – 80° .

a pure perovskite phase with tetragonal symmetry for all samples, indicating that Nb^{5+} successfully diffused into the lattice structure of the BNKT ceramics to form complete solid solutions. No significant changes or extra phases in the crystallographic structure were identified in the studied composition range.

Fig. 2 illustrates the FE-SEM micrographs of the polished and thermally etched surfaces of KNN-modified BNKT ceramics with $x=0$, 0.03, 0.07 and 0.10. All ceramics were uniformly distributed and tightly bound with homogeneous macrostructures of similar grain morphology. KNN had little influence on the microstructure of the BNKT ceramics. The grain size decreased slightly with an increase in the KNN concentration. Using a linear intercept method, the grain size was found to decrease from $0.8\ \mu\text{m}$ for $x=0$ to $0.6\ \mu\text{m}$ for $x=0.10$.

The temperature-dependent dielectric constant and loss of BNKT– x KNN ceramics with $x=0$, 0.03, 0.07, and 0.10 measured at different frequencies (1, 10, and 100 kHz) are presented in Fig. 3. Two dielectric anomalies were observed in the dielectric curves of the BNKT–KNN ceramics, which corroborate the dielectric behavior of BNT and BNT-based ceramics [3,6]. The first dielectric anomaly below 200°C is often designated as the depolarization temperature (T_d), where the ferroelectricity significantly decreases, while the other (T_m) where the dielectric constant (ϵ_m) maximizes. BNKT ceramics without KNN exhibited a sharp T_d peak, which shifted toward a lower temperature with increasing KNN concentration. It is generally accepted that the dielectric constant is related to domain alignment and domain structure. The decrease in T_d could be a consequence of ferroelectric order destabilization and the formation of a non-polar (NP) phase induced by the KNN addition [15–17]. This behavior was more apparent from the polarization hysteresis loops shown in Fig. 5. Similar behavior was observed in our recent investigations of Zr-modified BNKT

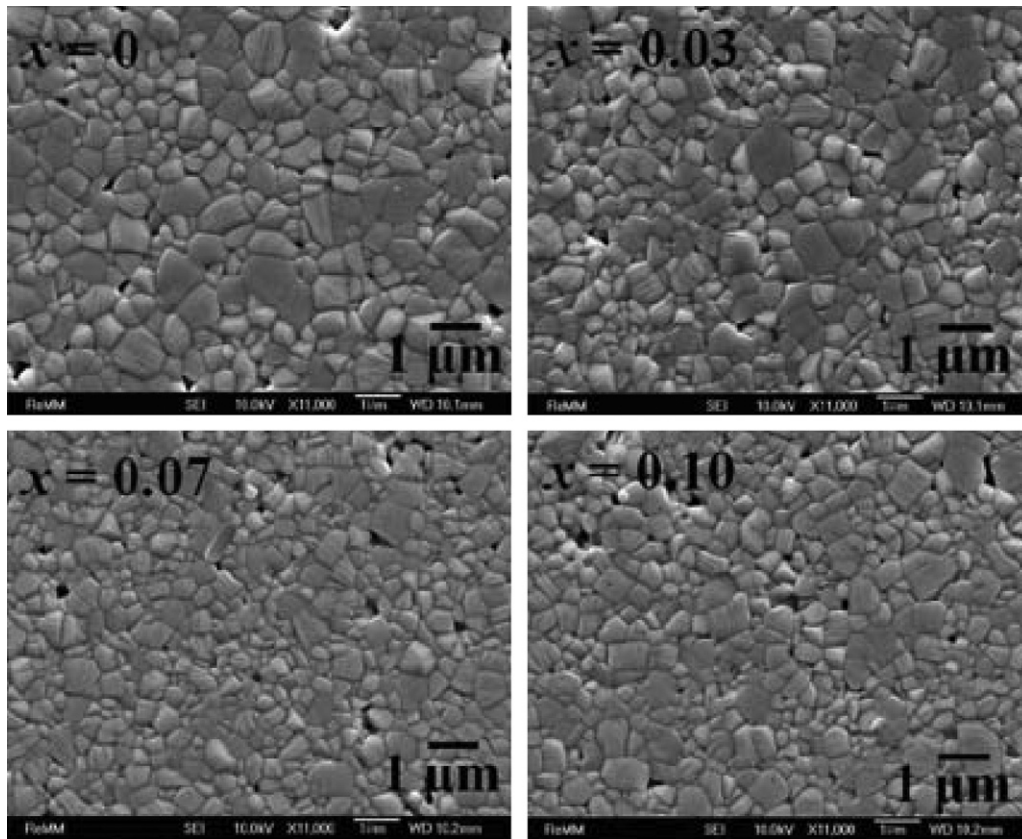


Fig. 2. FE-SEM micrographs of BNKT- x KNN ceramics with $x = 0, 0.03, 0.07$ and 0.10 .

ceramics [18], where T_d decreased with increasing Zr content in the BNKT ceramics, resulting in the stabilization of a NP phase. In addition, an increase in the KNN concentration gradually broadened the dielectric anomalies at T_d and T_m , suggesting that the KNN concentration induced a diffuse phase transition in the BNKT-KNN ceramics. A direct comparison of the dielectric

constant and loss of KNN-modified BNKT ceramics at 100 kHz is shown in Fig. 4. The maximum dielectric constant for pure BNKT was approximately 5400, which decreased to 3000 for 10 mol% KNN-modified BNKT ceramics. In addition, as KNN content increased from 0 to 0.10, T_d decreased from 110 to 75 °C and T_m decreased from 294 to 246 °C. The combination of

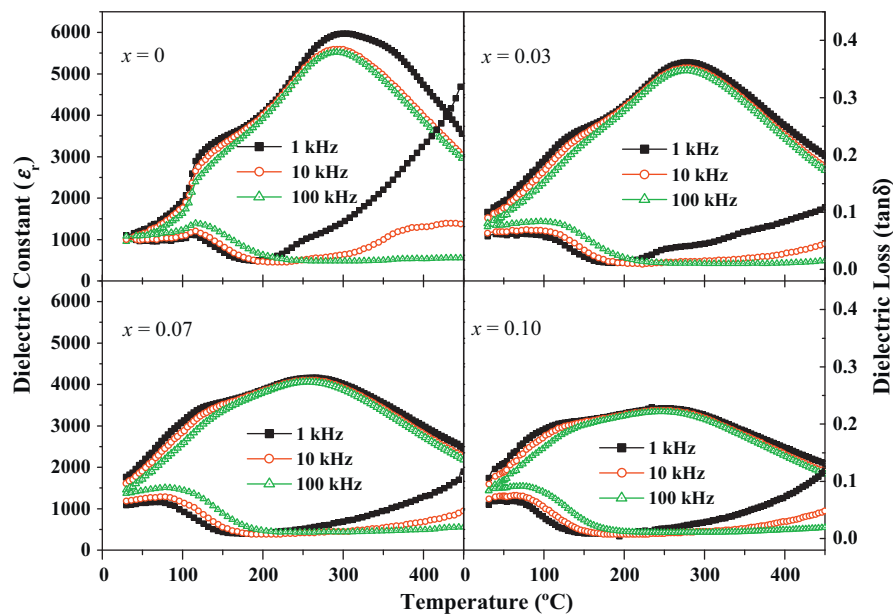


Fig. 3. The dielectric constant and loss of BNKT- x KNN ceramics as a function of temperature and frequency with $x = 0, 0.03, 0.07$, and 0.10 .

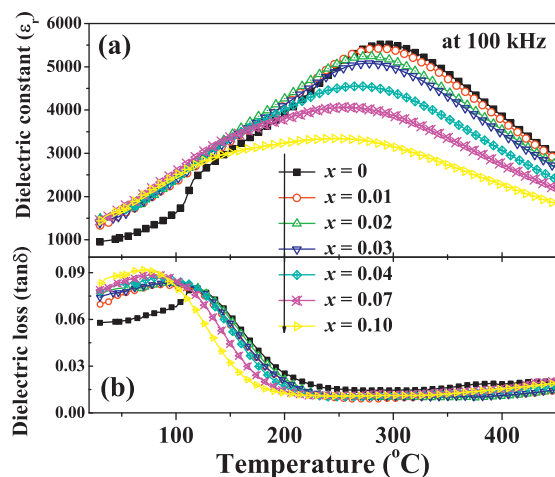


Fig. 4. Direct comparison of dielectric constants and loss of BNKT- x KNN ceramics as a function of temperature measured at 100 kHz.

diffuse character and the decrease in T_d and T_m in the KNN-modified BNKT ceramics may be due to Nb ion substitutions, which are the source of random fields that break the long range order of BNKT and stabilize the polar nanoregions at low temperature and zero field, similar to that proposed for BZT ceramics [19].

Fig. 5 shows the room temperature polarization versus electric field (P - E) hysteresis loops of the BNKT- x KNN ceramic with $x = 0, 0.03, 0.07$, and 0.10 measured at 2 Hz. Ceramics without KNN exhibited a typical polarization hysteresis loop with a remnant polarization (P_r) of $24 \mu\text{C}/\text{cm}^2$ and a coercive field (E_c) of $18 \text{ kV}/\text{cm}$. As shown in Fig. 5, KNN exerts significant influence on the loop shape and

polarization values. P_r and E_c steeply decreased with increasing KNN. However, at $x = 0.03$, the P_r drastically decreased from 24 to $11 \mu\text{C}/\text{cm}^2$, and the E_c decreased from 18 to $10 \text{ kV}/\text{cm}$. As a result, the hysteresis curve became slightly pinched and the maximum polarization did not change considerably. At higher KNN concentrations, $x \geq 0.05$, both P_r and E_c drastically decreased, indicating the material became electrostrictive without any apparent switching. This significant decrease in P_r and E_c along with concurrent minor decreases in P_m implies that the long-range ferroelectric order dominant in BNKT is disrupted with the addition of KNN. The characteristic values of P_r , P_m , their difference, $P_m - P_r$, and E_c are listed in Table 1.

To better understand the ferroelectric behavior of KNN-modified BNKT ceramics, the P - E loops were measured above room temperature. At high temperatures, the P - E loops of BNKT-KNN ceramics with $x \leq 0.03$ exhibited similar behavior to room temperature composition dependence. P_r , P_m , and E_c values decreased with an increase in temperature. In addition, a pinched-type character was also observed for samples with $x \leq 0.03$ at elevated temperatures (i.e., near T_d). For pure BNKT, a pinched-type loop can be observed at $75^\circ\text{C} \leq T \leq 150^\circ\text{C}$. However, this pinched-type characteristic can be observed at $50^\circ\text{C} \leq T \leq 100^\circ\text{C}$ for doped BNKT samples ($x \leq 0.03$). The pinched-type character in $x \leq 0.03$ KNN modified samples vanished and the loops took on the shape of linear dielectric materials at higher temperatures; 175°C for pure BNKT and 125°C for modified ceramics. Such behavior in the temperature-dependent P - E loops was also observed in other BNT-based materials [20–23]. Fan et al. [20] examined the temperature-dependent P - E hysteresis loops of the $\text{Bi}_{0.5}\text{Na}_{0.5}\text{TiO}_3$ - KNbO_3 ceramics and reported the existence

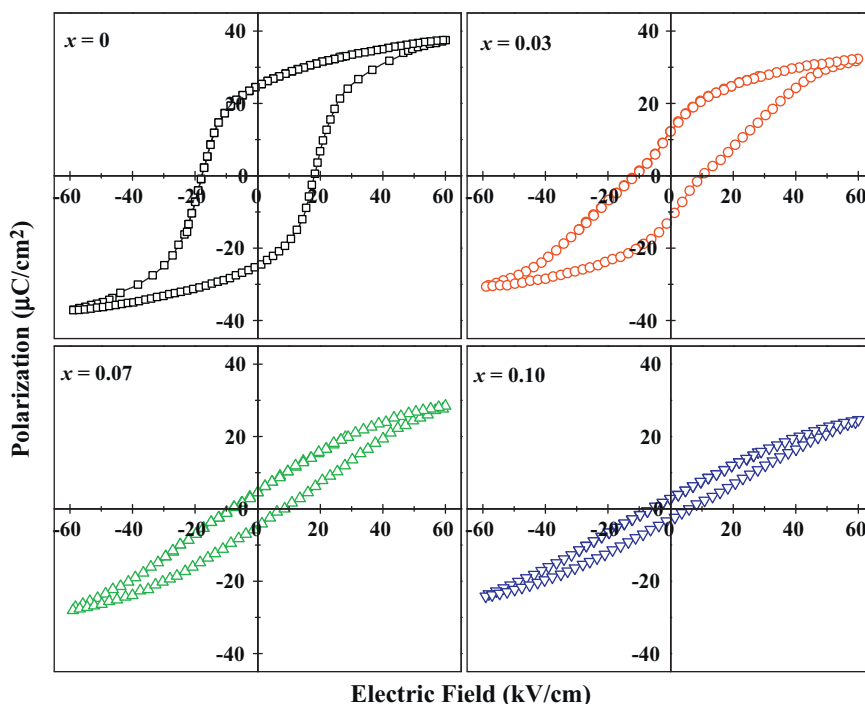


Fig. 5. Room temperature polarization hysteresis loops of the BNKT- x KNN ceramics with $x = 0, 0.03, 0.07$, and 0.10 .

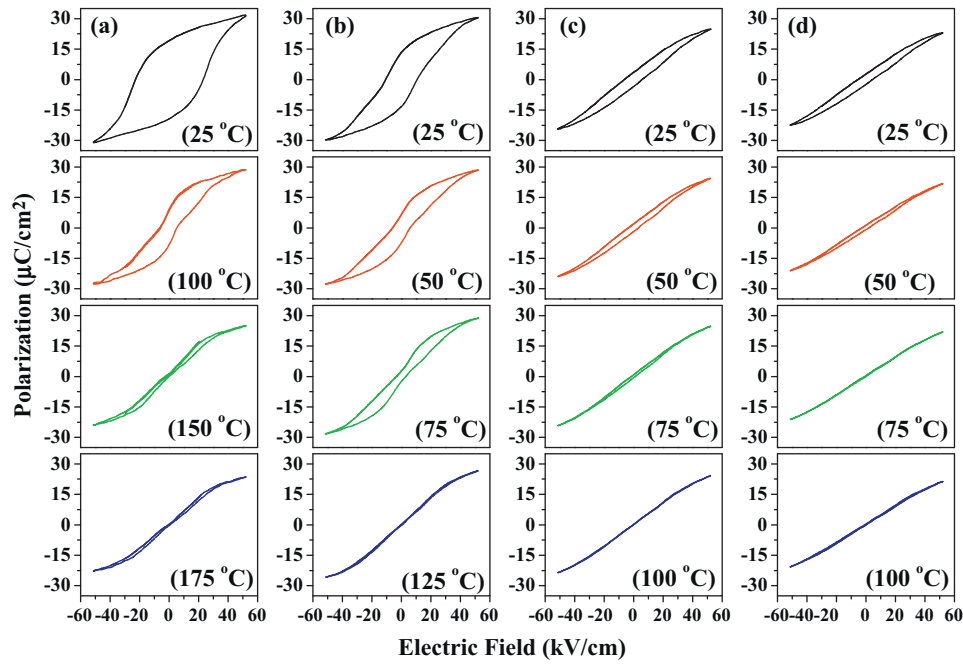


Fig. 6. P - E hysteresis loops of the BNKT- x KNN ceramics with $x = 0, 0.03, 0.07$, and 0.10 at different temperatures.

of a NP phase between T_d and T_c . Similarly, for $\text{Bi}_{0.5}\text{Na}_{0.5}\text{TiO}_3$ - BaTiO_3 - $\text{Bi}_{0.5}\text{Li}_{0.5}\text{TiO}_3$ [21] and $\text{Bi}_{0.5}\text{Na}_{0.5}\text{TiO}_3$ - SrTiO_3 - $\text{Bi}_{0.5}\text{Li}_{0.5}\text{TiO}_3$ [22], Lin et al. suggested the coexistence of polar and NP phases. Recently, Jo et al. [23] monitored the volume change in $\text{Na}_{0.5}\text{K}_{0.5}\text{NbO}_3$ -modified $\text{Bi}_{0.5}\text{Na}_{0.5}\text{TiO}_3$ - BaTiO_3 ceramics and proposed that the pinch-type character in the P - E loops originated from the existence of a NP phase. The pure BNKT sample showed typical FE character with a high P_r compared to that of KNN-modified BNKT ceramics shown in Fig. 5. KNN modification disrupted the FE order of the BNKT ceramics, leading to a decrease in the polarization states (P_r and P_m). These results suggest that the FE order of BNKT ceramics is transformed into an NP phase when Nb is substituted for Ti. At a higher concentration of KNN, the NP phase became dominant due to the significant reduction in the polarization states (P_m and P_r). Furthermore, along with polarization, the piezoelectric constant, d_{33} , also drastically decreased from 168 pC/N for pure BNKT to 9 pC/N for $x = 0.10$, as shown in Table 1. The drastic decrease in d_{33} at $x = 0.03$ can be explained by the thermodynamic theory of ferroelectrics [24]. According to this theory, d_{33} can be expressed as $d_{33} = 2Q_{11}P_r\epsilon_{33}^T$, where Q_{11} represents the electrostrictive coefficient, which is constant

for perovskite materials. P_r and ϵ_{33}^T represent the remnant polarization and dielectric constant of the material. d_{33} is proportional to P_r and the P_r value decreased at $x = 0.03$ from 24 $\mu\text{C}/\text{cm}^2$ for pure BNKT to 11 $\mu\text{C}/\text{cm}^2$, resulting in a significant reduction in d_{33} . At higher KNN concentrations ($x = 0.10$), the P_r is so small that a very small piezoelectric constant ($d_{33} = 9$ pC/N) is observed.

Fig. 7(a) shows room temperature bipolar field-induced strain curves of BNKT- x KNN ceramics for compositions $x = 0, 0.03, 0.07$, and 0.10 measured at 0.2 Hz under an applied electric field of 50 kV/cm. Pure BNKT ceramics without KNN exhibit a butterfly shaped curve typical of a ferroelectric material with maximum and negative strains of 0.12% and 0.11%, respectively. When a small amount of KNN is introduced, the curves change shape, resulting in an increase in maximum strain and a concurrent decrease in the negative strain. At 3 mol% KNN, a significant enhancement in strain ($S = 0.22\%$) was observed. However, above this critical composition ($x = 0.03$), drastic changes from the typical ferroelectric order were observed. This was evidenced by the absence of a negative strain, which is the difference between the zero field strain and the lowest strain and is closely related to

Table 1
Ferroelectric and piezoelectric properties of KNN-modified BNKT ceramics.

Comp. (x)	Density g/cm^3	E_c (kV/cm)	P_r ($\mu\text{C}/\text{cm}^2$)	P_m ($\mu\text{C}/\text{cm}^2$)	$P_m - P_r$ ($\mu\text{C}/\text{cm}^2$)	d_{33} (pC/N)	S_{\max} (%)	d_{33}^* (pm/V)
0	5.62	18	24	37	15	168	0.11	237
0.01	5.66	12	20	38	26	115	0.12	250
0.02	5.7	11	16	36	29	55	0.14	320
0.03	5.78	10	11	32	32	27	0.22	434
0.04	5.73	9	8	31	31	16	0.19	385
0.05	5.71	8.3	7	30	30	12	0.18	370
0.07	5.7	8	5	26	29	14	0.17	344
0.10	5.67	5	3	24	26	9	0.1	200

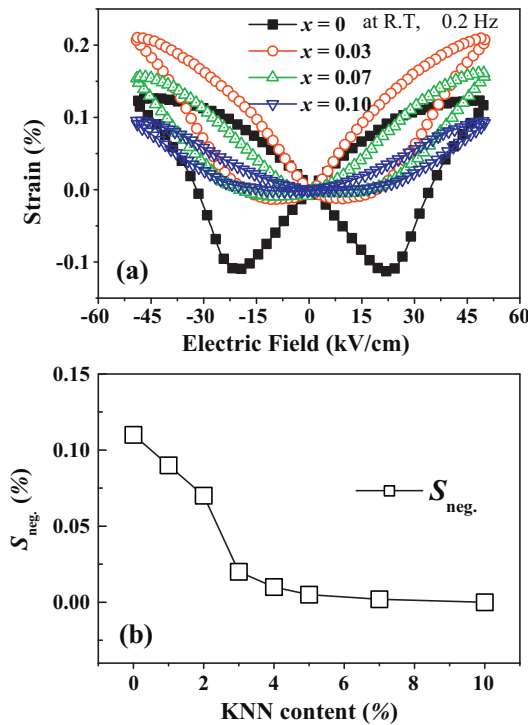


Fig. 7. (a) The bipolar field-induced strain curves of the BNKT- x KNN ceramics with $x = 0, 0.03, 0.07$, and 0.10 measured at 0.2 Hz. (b) Negative strain and piezoelectric coefficient of BNKT- x KNN ceramics as a function of KNN content.

domain back-switching during bipolar cycles [10]. The decreasing trend for the negative strain level ($S_{\text{neg.}}$) of BNKT- x KNN ceramics as a function of KNN content is depicted in Fig. 7(b). The significant enhancement in bipolar strain at $x = 0.03$ attributed to the NP to ferroelectric phase transition corroborates the polarization hysteresis loop (Fig. 6), where the pinched-type characteristic indicates the coexistence of ferroelectric and NP phases [10,15,16,18].

The unipolar electric field-induced strain curves of the BNKT- x KNN ceramics with $x = 0, 0.03, 0.07$, and 0.10 measured at room temperature are shown in Fig. 8(a). Similar to bipolar strain, unipolar strain increased significantly with increasing KNN content up to $x = 0.03$ and then decreased beyond this critical composition. The field-induced strain S_{max} (%) and normalized strain d_{33}^* of BNKT- x KNN ceramics as a function of KNN content are presented in Fig. 8(b). The enhanced strain ($S_{\text{max}} = 0.22\%$) nearly doubled that of pure BNKT and the normalized strain ($d_{33}^* = S_{\text{max}}/E_{\text{max}} = 434$ pm/V) was obtained for $x = 0.03$ at a relatively low applied electric field of 50 kV/cm. Recently, increased strain under a greater driving field has been achieved in BNT-based systems, such as BNT-BKT-KNN [15], BNT-BT-KNN [23], Hf-modified BNKT [25] and other modified BNT-BKT compositions [10–18]. However, the noticeable peculiarity in the present study is that the driving field was successfully reduced to 50 kV/cm, which indicates feasibility for practical applications.

KNN has good ferroelectric characteristics and pure BNKT exhibited typical ferroelectric order with large P_r and E_c values

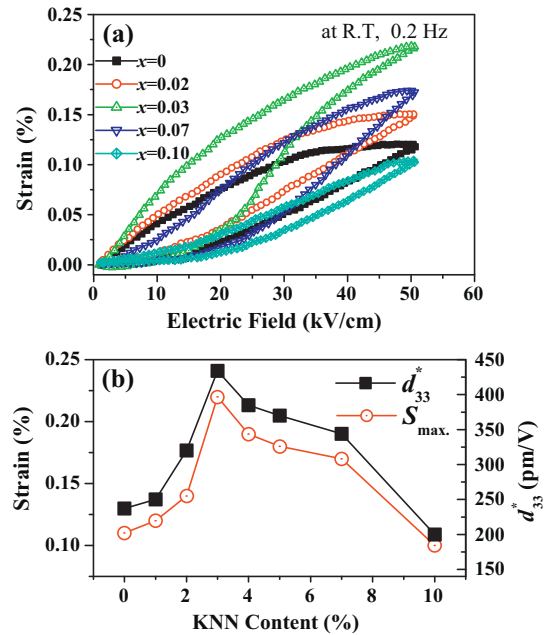


Fig. 8. (a) Unipolar field-induced strain curves of the BNKT- x KNN ceramics with $x = 0, 0.03, 0.07$, and 0.10 . (b) Maximum strain and normalized strain ($d_{33}^* = S_{\text{max}}/E_{\text{max}}$) as a function of KNN content in BNKT-KNN ceramics.

of $24 \mu\text{C}/\text{cm}^2$ and 18 kV/cm, respectively. However, the addition of KNN into a BNKT lattice disrupts the long-range ferroelectric order of pure BNKT ceramics, leading to a significant decrease in P_r and E_c values. The significant decrease in polarization values and noticeable change in the loop shape with increasing KNN content suggests that KNN induced a phase transition in the BNKT lattice from a ferroelectric (polar) to a NP phase, and passed through an intermediate stage that exhibits both ferroelectric and NP characteristics. The free energy of the ferroelectric phase was comparable to that of the NP phase under zero field, such that it can be easily induced by an external electric field and becomes saturated at 60 kV/cm, as shown in Fig. 5. Furthermore, the NP phase dominated at higher KNN concentrations (i.e., $x = 0.10$), which delays the transformation from the NP phase to the ferroelectric phase based on the significant decrease in the maximum polarization from 37 to $24 \mu\text{C}/\text{cm}^2$. The results of this study suggest that high unipolar strain, located only in a narrow region (i.e., near $x = 0.03$) in which both ferroelectric and NP phases coexist in the BNKT- x KNN ceramic system, exhibits competitive free energy. Beyond this narrow region, either the ferroelectric or NP phase dominates. Neither of the phases can solely deliver a strain as large as that measured from compositions ($x = 0.02$ – 0.04) near the boundary between polar and NP phases. The P - E hysteresis loops and S - E curves suggest that the large strain at $x = 0.03$ can be attributed to the coexistence of ferroelectric and NP phases.

4. Conclusion

The effect of KNN on dielectric, ferroelectric and piezoelectric properties of BNKT ceramics was investigated. XRD revealed that KNN addition had no remarkable effect on the

crystal structure of BNKT ceramics in the studied composition range. ϵ_m decreased and T_d shifted toward lower temperatures with increasing KNN concentration. Deformed hysteresis loops at small KNN concentrations were observed, suggesting the coexistence of polar and NP phases for modified BNKT ceramics. At 3 mol% KNN, a pinched-type hysteresis loop with low remnant polarization ($11 \mu\text{C}/\text{cm}^2$) and a small piezoelectric constant ($27 \text{ pC}/\text{N}$) was observed. Alternatively, the unipolar field-induced strain was enhanced from 0.11% for pure BNKT to 0.22% for 3 mol% of KNN under an applied electric field of 50 kV/cm, corresponding to a normalized strain ($S_{\text{max}}/E_{\text{max}}$) of 434 pm/V. This significant strain enhancement is a result of the reversible phase transition between a NP phase in a zero field and a field-induced ferroelectric phase.

Acknowledgements

This work was supported by Mid-career Researcher Program through NRF Grant (2011-0016790) funded by MEST and National Research Foundation of Korea Grant funded by the Korean government (2010-0015955).

References

- [1] L.E. Cross, Lead-free at last, *Nature* 432 (2004) 24–25.
- [2] Y. Saito, H. Takao, T. Tani, T. Nonoyama, K. Takatori, T. Homma, T. Nagaya, M. Nakamura, Lead-free piezoceramics, *Nature* 432 (2004) 84–87.
- [3] G.A. Smolenskii, V.A. Isupov, A.I. Agranivskaya, N.N. Krainik, New ferroelectrics of complex composition, *Sov. Phys.: Solid State* 2 (1961) 2651–2654.
- [4] Y. Hiruma, Y. Imai, Y. Watanabe, H. Nagata, T. Takenaka, Large electro-strain near the phase transition temperature of $(\text{Bi}_{0.5}\text{Na}_{0.5})\text{TiO}_3$ – SrTiO_3 ferroelectric ceramics, *Appl. Phys. Lett.* 92 (2008) 262904.
- [5] H. Nagata, T. Takenaka, Additive effects on electrical properties of $(\text{Bi}_{1/2}\text{Na}_{1/2})\text{TiO}_3$, ferroelectric ceramics, *J. Eur. Ceram. Soc.* 21 (2001) 1299–1302.
- [6] T. Takenaka, K. Maruyama, K. Sakata, $(\text{Bi}_{1/2}\text{Na}_{1/2})\text{TiO}_3$ – BaTiO_3 system for lead-free piezoelectric ceramics, *Jpn. J. Appl. Phys.* 30 (1991) 2236–2239.
- [7] A. Sasaki, T. Chiba, Y. Mamuya, E. Otsuki, Dielectric and piezoelectric properties of $(\text{Bi}_{0.5}\text{Na}_{0.5})\text{TiO}_3$ – $(\text{Bi}_{0.5}\text{K}_{0.5})\text{TiO}_3$ systems, *Jpn. J. Appl. Phys.* 38 (1999) 5564–5567.
- [8] Y. Hiruma, H. Nagata, T. Takenaka, Phase transition temperatures and piezoelectric properties of $(\text{Bi}_{1/2}\text{Na}_{1/2})\text{TiO}_3$ – $(\text{Bi}_{1/2}\text{K}_{1/2})\text{TiO}_3$ – BaTiO_3 lead-free piezoelectric ceramics, *Jpn. J. Appl. Phys.* 45 (2006) 7409–7412.
- [9] X.X. Wang, X.G. Tang, H.L.W. Chan, Electromechanical and ferroelectric properties of $(\text{Bi}_{1/2}\text{Na}_{1/2})\text{TiO}_3$ – $(\text{Bi}_{1/2}\text{K}_{1/2})\text{TiO}_3$ – BaTiO_3 lead-free piezoelectric ceramics, *Appl. Phys. Lett.* 85 (2004) 91.
- [10] S.T. Zhang, A.B. Kouna, E. Aulbach, T. Granzow, W. Jo, H.J. Kleebe, J. Rödel, Lead-free piezoceramics with giant strain in the system $\text{Bi}_{0.5}\text{Na}_{0.5}\text{TiO}_3$ – BaTiO_3 – $\text{K}_{0.5}\text{Na}_{0.5}\text{NbO}_3$. I. Structure and room temperature properties, *J. Appl. Phys.* 103 (2008) 034107.
- [11] L. Egerton, D.M. Dillon, Piezoelectric and dielectric properties of ceramics in the system potassium–sodium niobate, *J. Am. Ceram. Soc.* 42 (1959) 438–442.
- [12] L.E. Cross, Electric double hysteresis in $(\text{K}_x\text{Na}_{1-x})\text{NbO}_3$ single crystals, *Nature* 181 (1958) 178–179.
- [13] R.E. Jeager, L. Egerton, Hot pressing of potassium–sodium niobates, *J. Am. Ceram. Soc.* 45 (1962) 209–213.
- [14] Z. Yao, H. Liu, L. Chen, M. Caw, Morphotropic phase boundary and piezoelectric properties of $(\text{Bi}_{1/2}\text{Na}_{1/2})_{1-x}(\text{Bi}_{1/2}\text{K}_{1/2})_x\text{TiO}_3$ – $0.03(\text{Na}_{0.5}\text{K}_{0.5})\text{NbO}_3$ ferroelectric ceramics, *Mater. Lett.* 63 (2009) 547–550.
- [15] K.T.P. Seifert, W. Jo, R. Rödel, Temperature-insensitive large strain of $(\text{Bi}_{1/2}\text{Na}_{1/2})\text{TiO}_3$ – $(\text{Bi}_{1/2}\text{K}_{1/2})\text{TiO}_3$ – $(\text{K}_{0.5}\text{Na}_{0.5})\text{NbO}_3$ lead-free piezoceramics, *J. Am. Ceram. Soc.* 93 (2010) 1392–1396.
- [16] F. Wang, M. Xu, C.M. Leung, Y. Tang, T. Wang, X. Chen, W. Shi, Composition and temperature-induced structure evolution in $\text{Bi}_{0.5}\text{Na}_{0.5}\text{TiO}_3$ -based solid solutions, *J. Mater. Sci.* (2011), doi:10.1007/s10853-011-5796-x.
- [17] L.A. Schmitt, J. Kling, M. Hinterstein, M. Hoelzel, W. Jo, H.J. Kleebe, H. Fuess, Structural investigations on lead-free $\text{Bi}_{1/2}\text{Na}_{1/2}\text{TiO}_3$ -based piezoceramics, *J. Mater. Sci.* 46 (2011) 4368–4376.
- [18] A. Hussain, C.W. Ahn, J.S. Lee, A. Ullah, I.W. Kim, Large electric-field-induced strain in Zr-modified lead-free $\text{Bi}_{0.5}(\text{Na}_{0.78}\text{K}_{0.22})_{0.5}\text{TiO}_3$ piezoelectric ceramics, *Sens. Actuators A* 84 (2010) 84–89.
- [19] R. Farhi, M.E. Marssi, A. Simon, J. Ravez, A Raman and dielectric study of ferroelectric $\text{Ba}(\text{Ti}_{1-x}\text{Zr}_x)\text{O}_3$ ceramics, *Eur. Phys. J. B* 9 (1999) 599–604.
- [20] G. Fan, W. Lu, X. Wang, F. Liang, J. Xiao, Phase transition behaviour and electromechanical properties of $(\text{Na}_{1/2}\text{Bi}_{1/2})\text{TiO}_3$ – KNbO_3 lead-free piezoelectric ceramics, *J. Phys. D: Appl. Phys.* 41 (2008) 035403–035406.
- [21] D. Lin, K.W. Kwok, H.L.W. Chan, Structure and electrical properties of $\text{Bi}_{0.5}\text{Na}_{0.5}\text{TiO}_3$ – BaTiO_3 – $\text{Bi}_{0.5}\text{Li}_{0.5}\text{TiO}_3$ lead-free piezoelectric ceramics, *Solid State Ionics* 178 (2008) 1930–1937.
- [22] D. Lin, K.W. Kwok, H.L.W. Chan, Ferroelectric and piezoelectric properties of $\text{Bi}_{0.5}\text{Na}_{0.5}\text{TiO}_3$ – SrTiO_3 – $\text{Bi}_{0.5}\text{Li}_{0.5}\text{TiO}_3$ lead-free ceramic, *J. Alloys Compd.* 481 (2009) 310–315.
- [23] W. Jo, T. Granzow, E. Aulbach, J. Rödel, D. Damjanovic, Origin of the large strain response in $(\text{K}_{0.5}\text{Na}_{0.5})\text{NbO}_3$ -modified $(\text{Bi}_{0.5}\text{Na}_{0.5})\text{TiO}_3$ – BaTiO_3 lead-free piezoceramics, *J. Appl. Phys.* 105 (2009) 094102.
- [24] M.J. Haun, E. Furman, S.J. Jang, L.E. Cross, Thermodynamic theory of the lead zirconate–titanate solid solution system, part I: phenomenology, *Ferroelectrics* 99 (1989) 13–25.
- [25] A. Hussain, C.W. Ahn, A. Ullah, J.S. Lee, I.W. Kim, Effects of hafnium substitution on dielectric and electromechanical properties of lead-free $\text{Bi}_{0.5}(\text{Na}_{0.78}\text{K}_{0.22})_{0.5}(\text{Ti}_{1-x}\text{Hf}_x)\text{O}_3$, *Jpn. J. Appl. Phys.* 49 (2010) 041504.